

# Suppression of the Kondo Effect in a Quantum Dot by Microwave Radiation

Jeroen M. Elzerman, Silvano De Franceschi,  
David Goldhaber-Gordon <sup>\*</sup>, Wilfred G. van der Wiel,  
and Leo P. Kouwenhoven

*Department of Applied Physics and DIMEs, Delft University of Technology,  
PO Box 5046, 2600 GA Delft, The Netherlands*

*We have studied the influence of microwave radiation on the transport properties of a semiconductor quantum dot in the Kondo regime. In the entire frequency range tested (10–50 GHz), the Kondo resonance vanishes by increasing the microwave power. This suppression of the Kondo resonance shows an unexpected scaling behavior. No evidence for photon-sideband formation is found. The comparison with temperature-dependence measurements indicates that radiation-induced spin dephasing plays an important role in the suppression of the Kondo effect.*

*PACS numbers:* 72.15.Qm, 73.23.Hk, 85.30.Vw

## 1. INTRODUCTION

The Kondo effect stems from a macroscopic quantum coherent coupling between a localized magnetic moment and a Fermi sea of electrons. The local magnetic moment is screened by hybridization with the delocalized electron-spins, leading to the formation of a bound spin-singlet state. A many-body resonance in the density of states (DOS) appears at the Fermi energy, which strongly influences the conductance of the system at low temperatures. Above the Kondo temperature, thermal fluctuations destroy the coherence, resulting in a non-monotonic dependence of the conductance on temperature.

<sup>\*</sup>Present address: Department of Physics, Harvard University, 17 Oxford Street, Cambridge MA 02138.

The equilibrium Kondo effect has been studied extensively in metals containing a dilute concentration of magnetic impurities.<sup>1</sup> In addition, the dependence on bias voltage and magnetic field was studied in single magnetic impurities encapsulated in a tunnel barrier.<sup>2</sup> In recent years, also semiconductor quantum dot devices have been considered,<sup>3–7</sup> thanks to their high controllability. For instance, a gate voltage can be used to change the number of confined electrons, and hence switch the total spin of the dot between zero (even electron number) and one half (odd electron number). In this way the Kondo temperature can be tuned from arbitrarily small values to typically a few Kelvin.

In this paper we investigate the Kondo effect in a quantum dot under controlled microwave irradiation. This is motivated by several theoretical studies,<sup>8–13</sup> which, interestingly, make contradicting predictions. Assuming that radiation of frequency  $f$  does not lead to ionization of the dot and subsequent spin-decoherence, it is expected that sidebands will appear in the DOS, at multiples of  $hf$  away from the main Kondo resonance. These sidebands should be measurable as additional peaks in the differential conductance.

In contrast to these predictions, Kaminski, Nazarov and Glazman<sup>13</sup> have pointed out that even without ionization, absorption of radiation during a cotunneling process effectively flips the spin on the dot. This spin flip cuts off the sequence of spin-correlated tunneling processes that build up the Kondo resonance, thus giving rise to a finite lifetime of the spin-singlet state. Consequently the Kondo effect is suppressed.

Now the question becomes whether in an experiment where the microwave power is progressively increased, the sidebands are observable before the Kondo effect is destroyed completely. Incidentally, low-power external radiation of unclear origin has been pointed out as the dominant cause for dephasing in weak localization experiments at low temperatures.<sup>14</sup> One of these experiments was recently performed with open quantum dots under intentional microwave irradiation.<sup>15</sup> Photon sidebands have been observed in quantum dots weakly coupled to electron reservoirs.<sup>16</sup> It should be stressed that in these experiments tunneling is a very weak perturbation and coherence does not play a role. In the present paper we employ the techniques outlined in Ref. 16 to investigate the still unexplored effects of microwaves in the strong-tunneling Kondo regime.

## Suppression of the Kondo Effect by Microwave Radiation

### 2. THEORY

#### 2.1. DC Kondo Effect in Quantum Dots

In a quantum dot with an odd number of electrons, the total spin is necessarily non-zero, resulting in a magnetic moment localized on the dot. This moment can be screened when exchange of electrons is possible with a nearby reservoir, as shown schematically in Fig. 1a. The dot is simplified to just one energy level,  $\varepsilon_0$ , which in Fig. 1a is occupied by an electron with spin-up. Adding an electron increases the energy by the on-site Coulomb interaction,  $U$ . The dot is coupled to two reservoirs with electrochemical potentials  $\mu_L$  and  $\mu_R$ , via tunnel barriers characterized by the tunneling rates  $\Gamma_L$  and  $\Gamma_R$ .

In the situation of Fig. 1a first-order tunneling is blocked by Coulomb charging effects.<sup>17</sup> Nevertheless, an electron can tunnel off the dot through an intermediate virtual state, which costs an energy  $\sim U$  and is allowed only for a short time  $\sim h/U$ . The system returns to a low-energy state when an electron tunnels onto the dot. This can result in an effective spin-flip. When many of such spin-flip tunneling events via virtual states take place in a coherent way, the total spin state of the dot plus reservoirs becomes a singlet, i.e. the local moment is completely screened. This, in brief, is the Kondo effect.<sup>1</sup>

The charge fluctuations associated with these higher-order tunneling events lead to a broadening of the single-particle state  $\varepsilon_0$  by an amount  $h\Gamma = h(\Gamma_L + \Gamma_R)$ . In addition, spin fluctuations give rise to a narrow many-body resonance in the tunneling density of states, located at the Fermi energies of the reservoirs (see Fig. 1b). The width of this resonance gives the typical energy scale for the Kondo effect,  $\sim k_B T_K$ , where  $T_K$  is the Kondo temperature. In terms of dot parameters,  $k_B T_K \approx \sqrt{h\Gamma U} e^{\pi(\varepsilon_0 - \mu)(\varepsilon_0 + U - \mu)/2h\Gamma U}$ , with  $\mu = \mu_L = \mu_R$ .<sup>18</sup> At temperatures above  $T_K$ , the Kondo effect is destroyed by thermal fluctuations.

In the linear regime, the Kondo resonance results in an enhanced conductance, since the two reservoirs are always connected by a dot with a finite DOS at the Fermi energy. Applying a bias voltage,  $V_{sd}$ , leads to a finite lifetime of the spin-singlet state and thus to a suppression of the Kondo effect. Experimentally, this translates into a peak in the differential conductance,  $dI/dV_{sd}$ , centered around  $V_{sd} = 0$ .

#### 2.2. AC Kondo Effect in Quantum Dots

Photon-assisted tunneling experiments on quantum dots<sup>16</sup> have shown that microwave radiation can give rise to the formation of photon sidebands (see Fig. 1c). Instead of just one single-particle state at  $\varepsilon_0$ , additional states

are formed at  $\varepsilon_0 \pm nhf$ , where  $n$  is an integer referring to the number of absorbed or emitted microwave photons. The occupation of these sidebands depends on the intensity of the radiation. We will only consider low powers, such that  $n$  is restricted to 0 or  $\pm 1$ .

Several theoretical papers<sup>8–13</sup> have addressed the question what would happen if such experiments are repeated in the Kondo regime. The answer is not immediately clear since the Kondo effect arises from a spin-correlation between many subsequent tunneling events. The question arises whether or not photon-assisted tunneling breaks this coherence. Note that the formation of sidebands in the single-particle spectrum makes this problem resemble the multi-level Kondo problem.<sup>19,20</sup> If the spin-coherence is not affected, the sidebands lead to narrow satellites of the Kondo resonance, at energies  $\mu \pm hf$  (see Fig. 1d). These satellites should be observable in the  $dI/dV_{sd}$  characteristics as additional peaks at  $V_{sd} = \pm hf/e$ .

However, the radiation can also induce decoherence in the spin-state of the system. One mechanism is related to ionization of the dot; an electron can be excited from the dot to the reservoirs by absorbing a photon, if the frequency is high enough (i.e.  $hf > \mu - \varepsilon_0$ ). A different electron can then tunnel back onto the dot, but it has no spin-correlation with the previous electron. This gives rise to a finite lifetime of the spin-singlet state, leading to a suppression of the Kondo effect.<sup>10</sup> Experimentally, this problem can quite easily be circumvented by choosing  $f$  low enough such that ionization is not allowed (i.e.  $hf < \mu - \varepsilon_0$ ).

Another, more subtle, mechanism for spin-decoherence is spin-flip cotunneling,<sup>13</sup> which is illustrated in Fig. 1e. It again involves the absorption of a photon and a subsequent spin-flip, but the difference is that now the intermediate state is virtual. As a result, this process is possible regardless of the microwave frequency. It is therefore the dominant decoherence-mechanism due to radiation at low frequencies.

It is important to note that the lifetime of the satellite peaks in the differential conductance can be substantially smaller than that of the main Kondo peak. This results from the fact that the satellites are measured at finite bias, which allows for extra decoherence processes. The strength of the satellite peaks depends in a complicated way on various parameters, such as the microwave power, frequency and temperature. The question whether the satellites of the main Kondo resonance are observable in experiments is difficult to answer *a priori*.

## Suppression of the Kondo Effect by Microwave Radiation

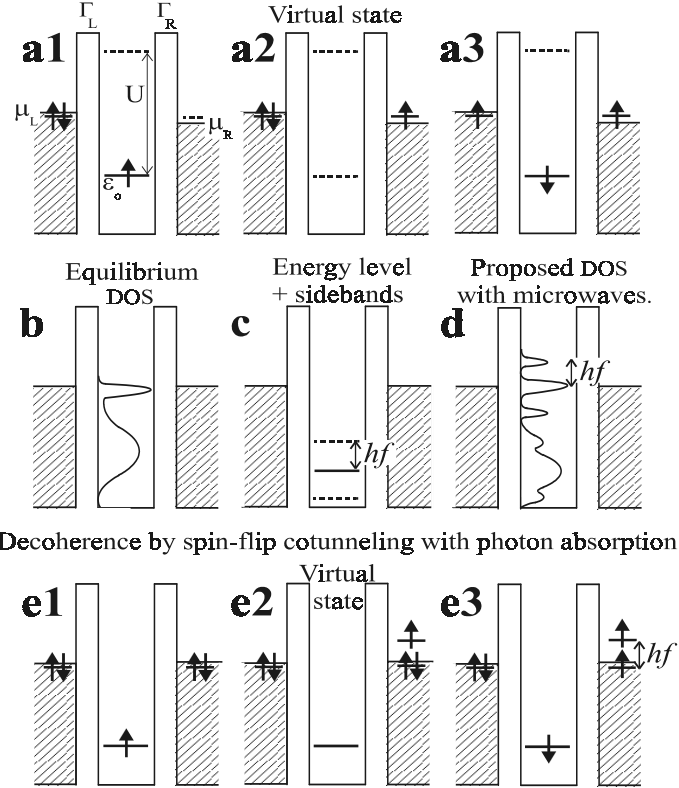


Fig. 1. (a) Energy diagrams with one spin-degenerate energy level  $\varepsilon_0$  occupied by a single electron. The series (a1, a2, a3) depicts an example of a higher-order tunneling event, in which the spin-up electron tunnels off the dot through a virtual intermediate state (a2), and a spin-down electron tunnels onto the dot. All such events involving spin-flips contribute to a macroscopically correlated state, the Kondo resonance. The resulting DOS is schematically shown in (b). The broad lower bump is due to  $\varepsilon_0$ , whereas the narrow peak at the Fermi energy of the leads represents the Kondo resonance. (c) In the presence of microwaves of frequency  $f$ , sidebands of the level  $\varepsilon_0$  develop at energies  $\varepsilon_0 \pm hf$ . (d) Besides these single-particle sidebands (the broad lower bumps in the DOS), microwaves may also lead to many-body satellites of the Kondo resonance (the narrow peaks at  $\mu \pm hf$ ). (e) Spin-flip cotunneling process involving the absorption of a photon. Such processes lead to spin decoherence.

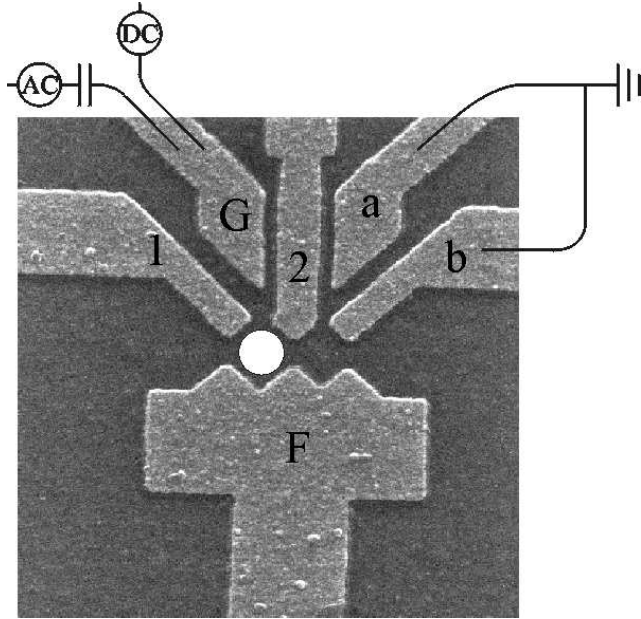


Fig. 2. SEM image of the quantum dot device. Light gray regions indicate the metallic gates, dark gray regions the surface of the GaAs/AlGaAs heterostructure. The white circle indicates the electron puddle. Both a DC and an AC voltage can be applied to the plunger gate G.

### 3. SAMPLE AND SETUP

An image of the device is shown in Fig. 2. Six metallic gates are fabricated on a GaAs/AlGaAs heterostructure containing a 2D electron gas (2DEG) about 100 nm below the surface. The electron density is  $1.9 \times 10^{15} \text{ m}^{-2}$ . Appropriate negative gate voltages define a small puddle of electrons, which is coupled to the 2DEG reservoirs via tunable tunnel barriers. The lithographic size of the dot is  $\sim 300 \times 300 \text{ nm}^2$ . Taking into account a depletion region, we estimate an effective size of about  $170 \times 170 \text{ nm}^2$  with approximately 60 electrons in the dot.

The two gates labelled *a* and *b* are grounded in the present experiments. Gates 1, 2 and *F* control the size of the dot and the tunnel barriers. A DC voltage,  $V_g$ , applied to the plunger gate, *G*, is used to finely tune the electron number. In addition, an AC voltage of amplitude  $V_\omega$  and frequency up to 50 GHz can be applied by coupling a high-frequency coaxial cable capacitively to the plunger gate. The AC power is controlled with a variable attenuator. Additional fixed attenuators are inserted in the coaxial line at

## Suppression of the Kondo Effect by Microwave Radiation

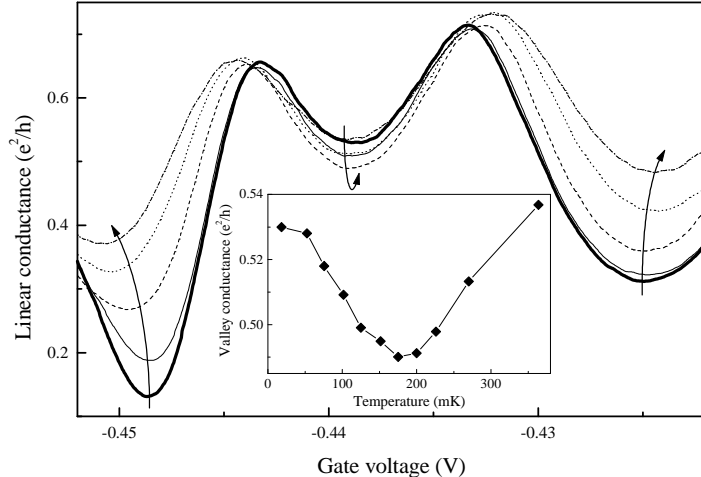


Fig. 3. Linear conductance,  $I/V_{sd}$ , versus gate voltage,  $V_g$ , for various temperatures:  $T$  (in mK) = 18 (thick), 102 (thin), 175 (dashed), 270 (dotted), 364 (dashed-dotted). Each curve has been given an offset in the x-direction to compensate for a temperature-dependent shift.<sup>21</sup> Arrows indicate the direction of increasing  $T$ . *Inset:* Conductance in the middle of the central valley versus temperature.

low temperatures. The effect of the microwaves is measured in DC transport. A current,  $I$ , is measured in response to a voltage,  $V_{sd}$ , applied between the source and drain reservoirs, using a standard lock-in technique with  $3 \mu\text{V}$  excitation at 17.7 Hz. The device was mounted in a dilution refrigerator, and temperature was varied between 18 mK and 600 mK. We have applied a magnetic field of 0.15 T, to lower the resistances of the Ohmic contacts. This field is small enough not to affect the Kondo resonance, i.e. the Zeeman splitting  $g\mu_B B \ll k_B T_K$ .

## 4. MEASUREMENTS

### 4.1. DC Kondo Effect

We make the tunnel barriers rather transparent, to increase the tunnel rate  $\Gamma$  and thus  $T_K$ . This leads to broad and overlapping Coulomb peaks, as in Fig. 3, which shows the linear conductance versus gate voltage for various temperatures between base temperature, 18 mK, and 365 mK.<sup>21</sup>

At base temperature (thick line), the two Coulomb peaks are paired. When the temperature,  $T$ , is raised, the conductance in the outer valleys increases (indicated by arrows). In the central valley, on the other hand, the

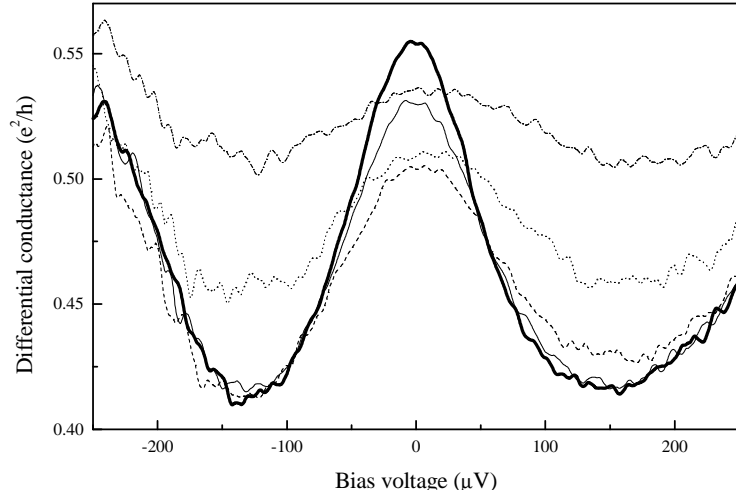


Fig. 4. Differential conductance,  $dI/dV_{sd}$ , versus bias voltage,  $V_{sd}$ , for various temperatures:  $T$  (in mK) = 18 (thick), 104 (thin), 154 (dashed), 203 (dotted), 285 (dashed-dotted). All traces are taken in the middle of the central valley in Fig. 3.

conductance first decreases until it starts to increase for  $T > 200$  mK. Also, the Coulomb peaks move apart. These are clear signs of the Kondo effect.

The Kondo zero-bias peak in  $dI/dV_{sd}$  is shown in Fig. 4 for various temperatures between 18 mK and 285 mK, and for  $V_g$  close to the middle of the central valley in Fig. 3. The increase in  $dI/dV_{sd}$  for  $|V_{sd}| > 150$   $\mu$ V corresponds to the threshold voltage to overcome the Coulomb energy  $U$ . When  $T$  is raised, the zero-bias peak decreases and becomes broader. At the same time, the “background” conductance goes up, due to thermally activated transport. As a result of these competing trends, the conductance at zero bias already starts to go up before the Kondo peak is fully suppressed. Even at 285 mK a small bump around zero bias remains visible.

Figure 5 shows the differential conductance on gray-scale versus both gate voltage and bias voltage. Because of the rather transparent tunnel barriers, the usual “diamond” shape of the Coulomb blockade regions cannot be distinguished very well. We estimate that the charging energy  $U = e^2/C \approx 500$   $\mu$ eV, a factor of three smaller than in the weak-tunneling regime.<sup>22</sup> The broadening of the single-particle states can be estimated from the width of the Coulomb blockade (CB) peaks;  $\hbar\Gamma \approx 200$   $\mu$ eV. The Kondo zero-bias peak is only present in the central valley, indicating that this valley corresponds to an odd number of electrons. The width of the peak yields  $k_B T_K \approx 100$   $\mu$ eV, or  $T_K \approx 1$  K. From measurements in the weak tunneling regime we find an effective electron temperature,  $T_{eff}$ , of about 70 mK. So,

## Suppression of the Kondo Effect by Microwave Radiation

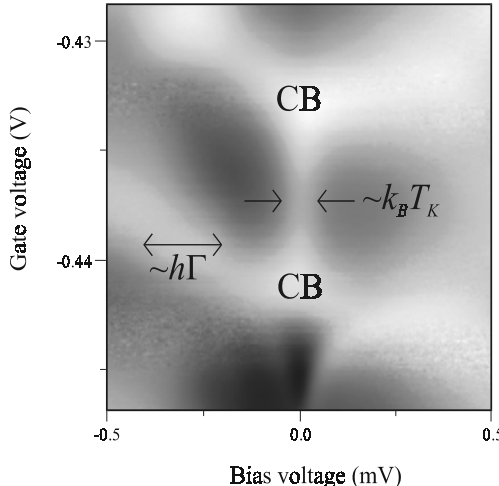


Fig. 5. Differential conductance in gray-scale versus gate voltage and bias voltage. In the darkest regions,  $dI/dV_{sd} \approx 0.35e^2/h$ , in the lightest regions  $dI/dV_{sd} \approx 0.7e^2/h$ . The broad diagonal lines correspond to the edge of the Coulomb gap. The thin line in the central valley along zero bias, which is absent in the adjacent valleys, represents the Kondo peak.

the thermal energy is  $k_B T_{eff} \approx 6 \mu\text{eV}$ , i.e. much smaller than the other energy scales.

### 4.2. Kondo Effect with Microwaves

The next step is to study the modification of the Kondo effect by microwave irradiation. We can apply frequencies up to 50 GHz, i.e. the photon energy  $hf$  can be tuned from 0 to about 200  $\mu\text{eV}$ . Figure 6a shows the linear conductance in the Kondo valley, as well as part of the two adjacent valleys, in the presence of microwaves of frequency 49.5 GHz. For this frequency,  $hf \approx h\Gamma \approx 2k_B T_K < U/2$ , which means that in the middle of the Kondo valley, the microwaves are not able to ionize the dot (i.e.  $hf < \mu - \varepsilon_0 \approx U/2$ ). In this case the dominant decoherence mechanism due to the microwaves is probably spin-flip cotunneling.

Different traces correspond to different intensities of the radiation. The thick curve is taken with an attenuation of -110 dB, which is essentially the same as without microwaves. If the power is increased, the two outer valleys go up, as indicated by the arrows, whereas the middle valley first comes

down and only goes up for the highest power. Also, we see that the two Coulomb peaks decrease and move apart. This behavior demonstrates that the microwaves suppress the Kondo effect; at a first glance in a similar way as increasing temperature.

Figure 6b shows a similar set of traces for a lower frequency  $f = 15.2$  GHz. Here the photon energy is considerably smaller than  $h\Gamma$  and  $U$  and of the same order as  $k_B T_K$ . Nevertheless, we observe virtually the same behavior as in Fig. 6a for 49.5 GHz, suggesting that the mechanism for the suppression of the Kondo effect is frequency independent.

The effect of microwaves on the Kondo peak in the differential conductance can be seen in Figs. 6c and 6d. The traces are taken in the middle of the Kondo valley. For increasing microwave power, the Kondo peak decreases and broadens. We do not observe any sidebands in the differential conductance. In Fig. 6c these should occur at  $V_{sd} = \pm hf/e = \pm 205 \mu\text{V}$  and in Fig. 6d at  $\pm 42 \mu\text{V}$ . Similar results were also obtained for  $f = 19.8$  GHz, 31.0 GHz and 41.9 GHz. This set of frequencies was chosen in order to cover different regimes, starting with  $hf$  being the smallest energy scale up to  $hf$  of order  $h\Gamma$ . The results are the same in all cases. In none of our measurements we have observed any indication of the formation of sidebands.

Besides these measurements in the middle of the Kondo valley, we have also studied the differential conductance more towards the right Coulomb peak. In this region  $hf > \mu - \varepsilon_0$  for  $f = 49.5$  GHz, such that ionization processes by microwaves are, in principle, possible. However, this did not seem to have a significantly different effect on the behavior of the Kondo peak as a function of microwave power. Also in this case, no evidence for sidebands of the Kondo resonance was found.

Figure 7a shows in detail the suppression of the Kondo zero-bias peak versus microwave attenuation. The lower axis gives the value of the applied attenuation. The upper axis gives the amplitude of the AC signal,  $V_\omega$ , relative to the amplitude without attenuation,  $V_0$ , on a logarithmic scale. The exact value of  $V_0$  cannot be determined, since we do not know the amplitude of the radiation as seen by the electrons in the dot. This depends not only on the applied attenuation, but also on the transmission for the frequency that is used. Although our high-frequency coaxial cable has a nearly flat frequency response, the coupling of the AC signal from coaxial cable via the capacitor and gate transmission line to the quantum dot is probably very frequency dependent.<sup>23</sup>

We can crudely estimate  $V_0$  in the following way; the microwaves start to have an effect when the amplitude of the energy oscillation exceeds the thermal fluctuations, i.e. when  $eV_\omega > k_B T_{eff} \approx 6 \mu\text{eV}$ . From Fig. 7a

## Suppression of the Kondo Effect by Microwave Radiation

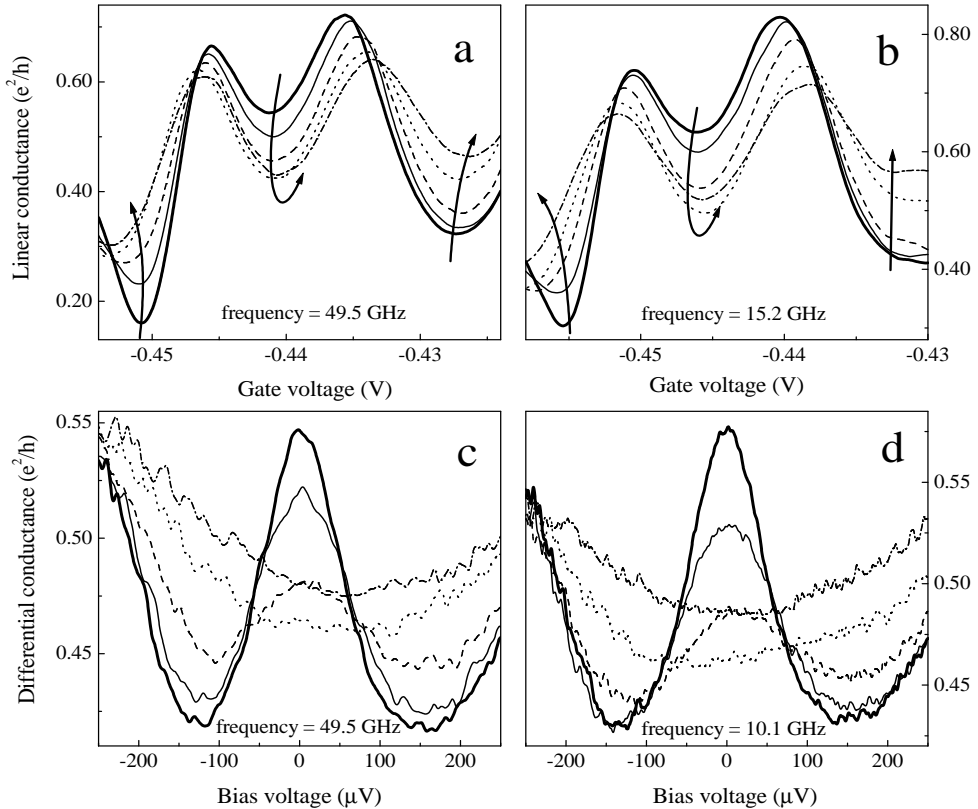


Fig. 6. Linear and differential conductance in the presence of microwaves of several frequencies. Different curves correspond to different values of the microwave intensity. Arrows indicate the direction of increasing microwave power. (a)  $f = 49.5$  GHz, attenuation (in dB) is equal to: -110 (thick), -20 (thin), -10 (dashed), 0 (dotted), +5 (dashed-dotted). (b)  $f = 15.2$  GHz, attenuation (in dB) is: -110 (thick), -50 (thin), -40 (dashed), -30 (dotted), -25 (dashed-dotted). (c) same as in (a). (d)  $f = 10.1$  GHz, attenuation (in dB) is: -110 (thick), -56 (thin), -46 (dashed), -36 (dotted), -26 (dashed-dotted). All differential conductance traces are taken in the middle of the Kondo valley. For the highest powers applied, multiple-photon absorption can not be ruled out.

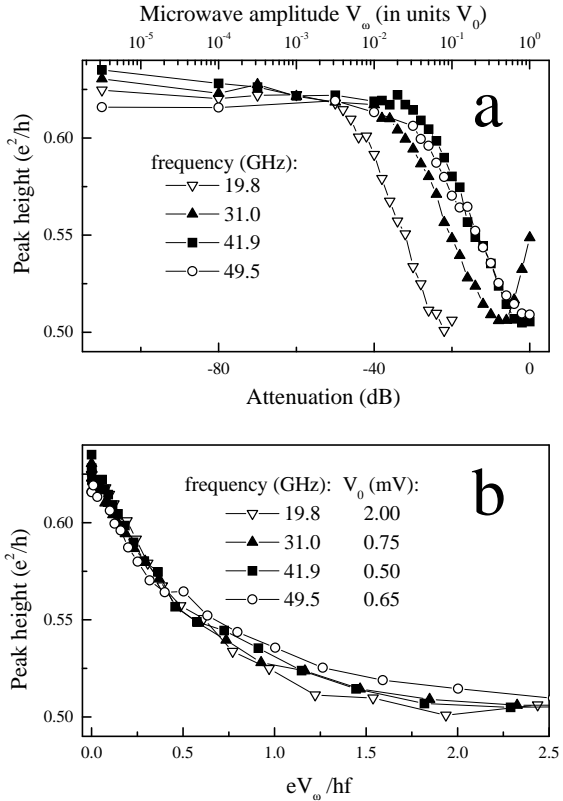


Fig. 7. (a) Height of the Kondo zero-bias peak versus microwave attenuation (lower scale). The upper scale gives the amplitude  $V_\omega$  of the AC signal in units of the frequency-dependent amplitude  $V_0$  without attenuation. (b) Same data, but now plotted versus  $eV_\omega/hf$ . The listed values of  $V_0$  correspond to the onset of peak-height suppression in panel (a). These parameters were slightly adjusted to obtain the best agreement between the different curves.

we find that for  $f = 19.8$  GHz the onset of the suppression occurs around  $V_\omega \approx 3 \times 10^{-3} V_0$ . Equating this to  $k_B T_{eff}/e$  gives  $V_0 \approx 2$  mV. With the same procedure we can also find  $V_0$  for the other frequencies. Using these values for  $V_0$  we obtain absolute values for the amplitude  $V_\omega$ , allowing us to replot the data of Fig. 7a against the dimensionless parameter  $eV_\omega/hf$ . From this procedure we find that curves taken at different frequencies nearly fall on top of each other. To illustrate this mapping most clearly we have allowed that  $V_0$  differs somewhat from the value obtained from the suppression onset in Fig. 7a. The results are shown in Fig. 7b on linear scales. As can be seen, we now obtain a scaling behavior for the Kondo peak height versus  $eV_\omega/hf$ . We note that this scaling behavior is not limited to the regime of

## Suppression of the Kondo Effect by Microwave Radiation

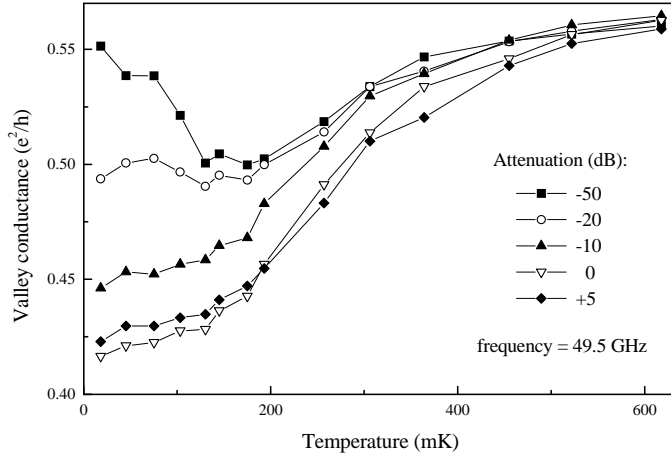


Fig. 8. Conductance in the middle of the Kondo valley versus temperature, in the presence of microwaves of different intensities.

weak power, i.e. the one-photon regime where  $eV_\omega/hf \ll 1$ .

We now compare the effect of temperature to the effect of microwaves in more detail. We note that in Fig. 6a the valley conductance decreases to  $0.43e^2/h$ , significantly smaller than  $0.49e^2/h$ , which is the lowest conductance in the  $T$ -dependence of Fig. 3. The same difference can also be seen in the differential conductance plots. In Fig. 4 the zero-bias conductance starts to rise before the Kondo peak is completely suppressed, whereas in Fig. 6b the curve with the lowest zero-bias conductance is essentially flat. This suggests that the Kondo effect is suppressed more efficiently by microwaves than by temperature. In other words, we cannot exactly translate microwave power to an “effective temperature”. This is to be contrasted with the conclusions of Ref. 15, where the effect of microwave radiation was indistinguishable from heating.

This also follows from Fig. 8, which shows the conductance in the middle of the Kondo valley versus temperature, in the presence of microwaves of various intensities. For the lowest intensity (-50 dB attenuation), the anomalous Kondo temperature-dependence is observed; first the conductance decreases to about  $0.5e^2/h$  at 200 mK, and then it starts to increase. For the curve with -20 dB attenuation, the conductance is already  $\sim 0.5e^2/h$  at base temperature. It remains more or less constant up to 200 mK, and then follows the -50 dB curve. However, by increasing the microwave power even more, we can suppress the conductance to a value substantially lower than  $0.5e^2/h$ . This is not possible by only raising the temperature, which again demonstrates the difference between heating and microwaves. At high temperatures, all curves essentially merge together. In this region, the effect

of the microwaves is negligible compared to temperature.

## 5. CONCLUSIONS

We have studied the modification of the Kondo effect in a quantum dot by microwave radiation. We have performed measurements over a range of temperatures, microwave frequencies, and power in order to cover the different regimes for photon-assisted tunneling processes. In all these measurements we find no indication for photon-induced sidebands to the Kondo resonance. The presence of microwaves suppresses the Kondo effect for all our frequencies. A detailed comparison shows that the microwave-induced suppression is different from the suppression by higher temperatures. We find an interesting scaling behavior; the Kondo resonance decreases with the dimensionless parameter  $eV_\omega/hf$  independently of frequency.

We believe that the observed suppression is due to a microwave-induced decoherence of the Kondo resonance by spin-flip cotunneling processes. For a definite conclusion it is necessary to perform a detailed comparison with numerical results on the microwave-induced dephasing of the Kondo resonance at finite temperature. Such a numerical study is presently being performed.<sup>25</sup>

## ACKNOWLEDGMENTS

We thank Yu. V. Nazarov, L. I. Glazman, A. Kaminski, R. Aguado, R. López, and G. Platero for useful discussions. This work was supported by the Dutch Organization for Research on Matter (FOM), and by the EU via the TMR network.

## REFERENCES

1. A. C. Hewson, *The Kondo Problem to Heavy Fermions* (Cambridge University Press, Cambridge, 1993).
2. J. M. Rowell, in *Tunneling Phenomena in Solids*, edited by E. Burstein and S. Lundquist (Plenum, New York, 1969), p. 385.
3. D. Goldhaber-Gordon, H. Shtrikman, D. Mahalu, D. Abusch-Magder, U. Meirav, and M. A. Kastner, *Nature* **391**, 156 (1998).
4. S. M. Cronenwett, T. H. Oosterkamp, and L. P. Kouwenhoven, *Science* **281**, 540 (1998).
5. D. Goldhaber-Gordon, J. Göres, M. A. Kastner, H. Shtrikman, D. Mahalu, and U. Meirav, *Phys. Rev. Lett.* **81**, 5225 (1998).
6. J. Schmid, J. Weis, K. Eberl, and K. von Klitzing, *Physica* (Amsterdam) **256B-258B**, 182 (1998).
7. F. Simmel, R. H. Blick, J. P. Kotthaus, W. Wegscheider, and M. Bichler, *Phys. Rev. Lett.* **83**, 804 (1999).

## Suppression of the Kondo Effect by Microwave Radiation

8. M. H. Hettler, and H. Schoeller, *Phys. Rev. Lett.* **74**, 4907 (1995).
9. T.-K. Ng, *Phys. Rev. Lett.* **76**, 487 (1996).
10. P. Nordlander, N. S. Wingreen, Y. Meir, and D. C. Langreth, *cond-mat/9801241*.
11. R. López, R. Aguado, G. Platero, and C. Tejedor, *Phys. Rev. Lett.* **81**, 4688 (1998).
12. Y. Goldin, and Y. Avishai, *Phys. Rev. Lett.* **81**, 5394 (1998).
13. A. Kaminski, Yu. V. Nazarov, and L. I. Glazman, *Phys. Rev. Lett.* **83**, 384 (1999).
14. B. L. Altshuler, M. E. Gershenson, and I. L. Aleiner, *Physica E* **3**, 58 (1998), also in *cond-mat/9803125*.
15. A. G. Huibers, J. A. Folk, S. R. Patel, C. M. Marcus, C. I. Duruöz, and J. S. Harris, Jr., *cond-mat/9904274*.
16. T. H. Oosterkamp, W. G. van der Wiel, S. De Franceschi, C. J. P. M. Harmans, and L. P. Kouwenhoven, *cond-mat/9904359*.
17. L. P. Kouwenhoven, C. M. Marcus, P. L. McEuen, S. Tarucha, R. M. Westervelt, and N. S. Wingreen, *Electron transport in quantum dots*, in *Mesoscopic Electron Transport*, edited by L.L. Sohn, L. P. Kouwenhoven, and G. Schön, (Kluwer, Series E 345, 1997), p. 105-214.
18. F. D. M. Haldane, *Phys. Rev. Lett.* **40**, 416 (1979).
19. T. Inoshita, A. Shimizu, Y. Kuramoto, and H. Sakaki, *Phys. Rev. B* **48**, 14725 (1993).
20. T. Pohjola, J. König, H. Schoeller, G. Schön, *Phys. Rev. B* **59**, 7579 (1999).
21. Each of the traces in Fig. 3 has been given an appropriate offset in the x-direction, to compensate for a  $T$ -dependent shift of all features towards more negative  $V_g$ . The shift is related to our “gate-voltage dividers”, consisting of two resistors attached to each gate (10  $M\Omega$  to ground and 40  $M\Omega$  to the gate voltage source), thermally anchored to the mixing chamber of the dilution refrigerator. They provide a low-temperature division of the gate voltage. Due to a  $T$ -dependence of the resistors between roughly 100 mK and 600 mK, the division factor is not always exactly equal to 5 but varies up to 10%. Recently we have checked that without the gate voltage dividers, no  $T$ -dependent shift occurs.
22. T. H. Oosterkamp, T. Fujisawa, W. G. van der Wiel, K. Ishibashi, R. V. Hijman, S. Tarucha, and L. P. Kouwenhoven, *Nature* **395**, 873 (1998).
23. An extremely frequency-sensitive phenomenon is “pumping”.<sup>16</sup> If the AC voltage drop over the two barriers is slightly asymmetric, the microwaves lead to a net current even for  $V_{sd} = 0$ ; i.e. the dot acts as an electron pump. Both the value and the polarity of the pumping current depend very sensitively on  $f$ . We attribute this to standing waves in the sample holder. We use frequencies that do not produce a pumping current. In this case, the microwave field does not induce an oscillating source-drain bias voltage.
24. The  $T$ -shift<sup>21</sup> was not present in this case. Intense microwaves can heat the electron system, but they do not heat the mixing chamber directly, so they do not affect the gate-voltage dividers.
25. R. López, R. Aguado, and G. Platero, private communication.